Nigerian Journal of Applied Physics (NJAP)
ISSN Print: 3115-5871
ISSN Online: 3115-588X
DOI: https://doi.org/10.62292/njap-v2i2-2026-89
Volume 2(2), June 2026

Application of 2-D Spectral Inversion and 3-D Standard Euler Deconvolution of Magnetic Anomalies over Subsurface Structures in Ilorin, Nigeria

*[1]Yusuf Magaji, [2]Timothy A. Kola, [3]Umar Issa, [4]Folorunsho O. Wahab, [5]Abdulsemiu O. Aina, [6]Hakeem I. Kuforiji and [7]Nicholas O. Anie

[1]Department of Geophysics, University of Ilorin, Ilorin, Kwara State, Nigeria.
[2]Department of Physics, Usmanu Danfodiyo University, Sokoto State, Nigeria.
[3]Department of Geology and Mineral Science, Kwara State University Malete, Kwara State, Nigeria.
[4]Geological Technology Department, Federal Polytechnic Offa, Kwara State, Nigeria.
[5]Department of Physics and Material Science, Kwara State University Malete, Kwara State, Nigeria.
[6]Department of Physics with Electronics, FUNAB, Iragbiji, Osun State, Nigeria.
[7] Department of Physics, Federal School of Surveying, Oyo State, Nigeria.

[*]Corresponding author's email: magajiyusuf30@gmail.com
ORCID: 0000-0001-6131-6242

ABSTRACT
The utilization of high-resolution aeromagnetic data in the geological interpretation of the basement complex of Ilorin has provided crucial insights into the spatial distribution and characteristics of magnetic anomalies, aiding in the delineation of structural discontinuities and the estimation of depths to anomalous bodies. This study explores the relationship between magnetic responses and geological features by employing 2-D spectral inversion and 3-D Standard Euler Deconvolution methods for depth estimation. Analysis of the aeromagnetic data reveals distinct magnetic zones within the study area, with varying intensities indicative of different lithological units such as migmatite, quartzite, biotite gneiss, and silicified quartz. Linear and curvilinear magnetic anomalies with sharp gradients are identified, suggesting the presence of structural features like faults and fractures possibly resulting from tectonic activity. The depth estimates to anomalous magnetic bodies range from 0.20 km to 1.10 km, with two-layer depth models (h1 and h2) representing shallower magnetic sources and the magnetic basement rock, respectively. The depth to the basement complex varies spatially, with the shallowest basement observed in the southern part of Ilorin and thicker sediment piles in the southwestern part. Overall, the estimated depths to basement range between 0.250 km and 0.480 km is characterized as the shallow depth for mineralization area. The findings identified faults and fractures that are significant for mineral potential assessment and geological mapping of the region.

Keywords:
Magnetic Anomaly,
Spectral Inversion,
Euler Deconvolution,
Structural Features.

INTRODUCTION

Airborne magnetic data have been used to delineate structural discontinuities and to determine the depth to anomalous bodies, and this has gained wide acceptability as it has evolved from its use solely for interpreting basement structures to conducting detailed examinations of lithologies and their spatial distributions (Magaji and Sanusi 2022; Chibuke *et al.*, 2022; Saheed and Magaji 2022). The use of magnetic surveys in showing the spatial distribution and relative abundance of magnetic and non-magnetic minerals in the upper crust is necessary. This technique aids in visualizing the geology and structural grains of the Earth's upper crust. Consequently, it enhances our understanding of the geological composition and structural features at these levels (Folorunso *et al.*, 2024; Olatunji and Warith, 2022; Salawu *et al.*, 2019; Falebita, 2008; Gun, 1997).

Several authors have used spectral inversion techniques in the determination of magnetic depth elsewhere (Saada, 2016; Udensi and Osazuwa, 2004; Opara *et al*., 2019; Magaji *et al.*, 2025a). Various techniques, based on the frequency analysis of the magnetic field, have been established by these authors to define parameters such as location of boundaries and depths of the magnetic rocks that cause anomalies in the magnetic field but the combination of spectral analysis and Euler deconvolution in identifying subsurface geologic structures and depth to the magnetic rocks that form the basement beneath the overlying non-magnetic rocks, sediments and soil that may offer a guide for future mineral exploration projects are yet to be conducted.

Similarly, Euler deconvolution method examines the shape of the magnetic field within a window and calculate the three-dimensional source locations based on the various magnetic structural index values (MSI). The structural index describes the rate at which the potential field decays based on source geometry and is specified based on expected target geometry. The knowledge of sedimentary overburden thickness is vital especially for the exploitation of ore minerals.

Depth to anomalous magnetic source interpretation provides clue to the basement complex architecture for the presence of minerals. The geological interpretation of the high resolution aeromagnetic data of the study area will further provide additional clarification of the basement depth, structural and tectonic history and mineral potential assessment of the study area This paper therefore presents the detailed interpretation of the airborne magnetic data over Ilorin area of the Nigerian basement complex with the objectives of mapping the geological features associated with the study area as well as the estimation of depth to anomalous magnetic bodies by incorporating 3-D Euler deconvolution and 2-D spectral methods. The integration of these methods helps to identify subsurface geologic structures and source depths that may be important in future mineral exploration and t is believed that the findings of this research will provide a classy knowledge base through which further exploration researches could be built on.

Geology of Study Area

The study area covers a half (1/2) degree sheet 223 bounded by latitudes 8°00′ and 8°30′N and longitudes 4°30′ and 5°00′E (Fig. 1). Detailed mapping of both surface and subsurface lithology involving the delineation of related structural features, interpretation of basement tectonics and dynamics in the study area were carried out. According to the detailed studies conducted by the Nigerian Geological Survey Agency (NGSA 2006), the area is underlain by the basement complex rocks of the northcentral Nigerian covering an area of about 3,080 km^2 (Figs. 2). Prominent rocks in the area include Granite gneiss, Biotite and biotite-hornblende gneiss, Migmatitic gneiss, Granite Gneiss, Augen Gneiss, Amphibole schist and amphibolite, Mica schist, Quartz schist, Silicified shear zone, Quartz vein, and Pegmatite (Fig. 2). These basement rocks were unconformably overlain by metasediments, and were then deformed, folded, and intruded by the Pan African Older granite suites.

It is believed that the basement rocks have been affected by at least 4 major orogenic cycles, involving deformation, metamorphism, and remobilization, associated with the Liberian (2,700 Ma), Eburnean (2,000 Ma), Kibaran (1,100 Ma), and Pan-African (600 Ma) events. The first three cycles showed intense deformation and isoclinal folding, along with regional metamorphism, followed by extensive migmatization (Rahaman, 1988). The Pan-African deformation brought regional metamorphism, migmatization, extensive granitization, and gneissification. These processes produced syntectonic granites and homogeneous gneisses (Abaa 1983). The formation of Nigerian rare-metal pegmatites occurred over a period from 562 to 534 Ma (Matheis and Caen Vachette, 1983; Rahaman, 1989), marking the waning stage of the Pan-African magmatic activity.

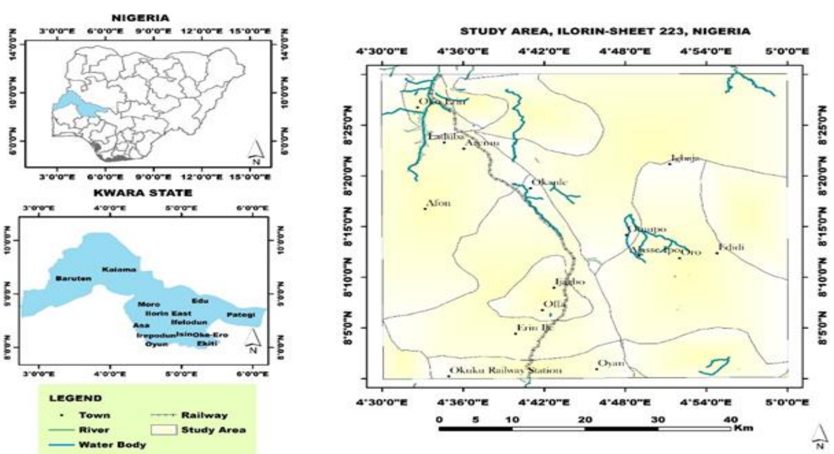

Figure 1: Location and accessibility maps of Ilorin (Sheet 223) (adapted from NGSA 2010)

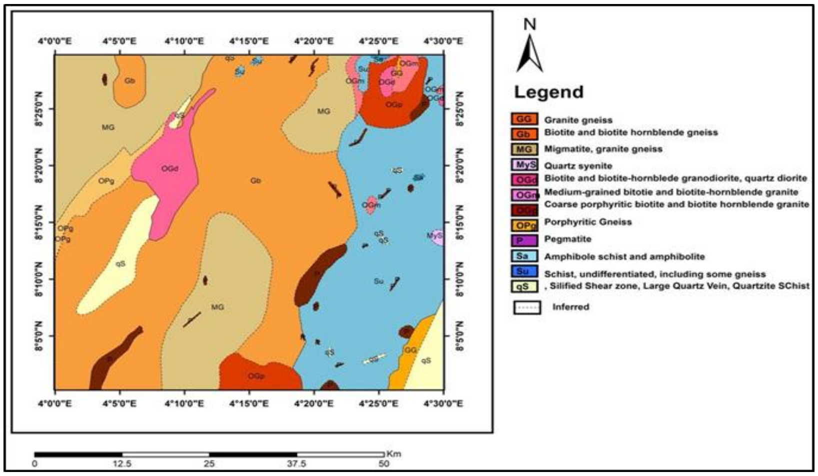

Figure 2: Geology map of Ilorin Area (Adapted from Nigerian Geological Survey Agency, 2006)

MATERIALS AND METHODS

The soft copy of digital high-resolution aeromagnetic data of Ilorin (Sheet 223) processed for this study was acquired from 2007 to 2008 by FUGRO Nig. Ltd in collaboration with the Nigerian Geological Survey Agency (NGSA). Flight line direction was NW-SE whereas the tie lines were NE–SW at station spacing of 0.5 km with flight line spacing of 0.5 km at a nominal flight altitude of about 80 m terrain clearance and tie line spacing of 2000 m. The airborne survey data were published in the form of 0.5° by 0.5° grid maps of total magnetic intensity (TMI) on a scale of 1:100,000. For ease of processing, the data was stripped of a common value of 33,000 nT. This value may therefore be added to every data point to get the exact regional field. However, doing this will not change the grid in any way since the value is common to all the data points. Data collection for this area was done between 2007 and 2008, so a 2007 epoch International Geomagnetic Reference Field (IGRF) was used to calculate inclination and declination as follows: Field strength = 33029.4393 nT; inclination = -8.25763595; declination = -2.63752396. The nature of filtering applied to the aeromagnetic data in this study was chosen to eliminate certain wavelengths and to pass longer wavelengths. Analytical methods used include 2-D spectral inversion and 3-D Euler deconvolution. The main software used for the processing and enhancement of the aeromagnetic were: Geosoft Oasis Montaj (version 8.4), Esri ArcGIS.

The 3D Euler Deconvolution method

Standard 3-D Euler method is based the potential field produced by many simple sources obeys Euler's homogeneity equation (Liu, 2003). This equation relates the potential Field (magnetic) and its gradient components to the location of the sources, by the degree of homogeneity (N), which can be interpreted as a structural index (Thompson, 1982). The method makes use of a structural index in addition to producing depth estimates. Simultaneous use of the depth estimates, and structure indices have the potential to calculate depth and determine the geological structures such as: faults, magnetic contacts, dykes, sills, etc. Although extensions to the Euler method allow for the estimation of SI from the data (Nabighian and Hansen, 2001), for thin 2D (two-dimensional) dyke structures an SI of 1 yields the best estimates (Reid *et al*., 1990). The algorithm uses a least squares method to solve Euler's equation simultaneously for each grid position within a sub-grid (window). A square window of pre-defined dimensions (number of grid cells) is moved over the grid along each row (Reid and Thurston, 2014). At each grid point, a system of equations is solved from which the four unknowns (x, y as location in the grid, z as depth estimation and the background value) and their uncertainties (standard deviation) are obtained for a given structural index. If a given component of the anomalous magnetic field ΔT (x; y; z) satisfies:

$$\Delta T\,(tx;\ ty;\ tz) = t^n\, \Delta T\,(x;\ y;\ z) \qquad (1)$$

Where n is the degree of homogeneity, then by differentiating equation (1) with respect to t, it can be shown that:

$$x\,\frac{\delta \Delta T}{\delta x} + y\,\frac{\delta \Delta T}{\delta y} + z\,\frac{\delta \Delta T}{\delta z} = n\Delta T \qquad (2)$$

Where, x, y and z are the coordinates of field observation points and source is assumed to be at the origin. The Euler homogeneity equation (equation 2) shows that the degree of homogeneity is source dependent and characterizes how fast the field decreases as a function of distance to the source (Reid *et al.*, 1990; Thompson, 1982). The function ΔT (x; y; z) can have a general function form (Whitehead, 2008).

$$\Delta T\,(x;\ y;\ z) = \frac{G}{r^N} \qquad (3)$$

Where $r^2 = (x - {x_0}^2) + (y - {y_0}^2) + (z - {z_0}^2)$, N is a real number (1, 2, 3.) and G a constant (independent of x, y, z). Many simple point magnetic sources can be described by equation 6 above, with $(x_0; y_0; z_0)$ the position of the source whose field F is measured. Since the potential field is inversely proportional to the distance raised to some power, the degree of homogeneity is non-positive. The negative of the degree of homogeneity is defined as the structural index (SI) and will be denoted as N. Table 1 gives a summary of the structural indices (SI) for some known geologic models. The number of infinite dimensions describes the extension of the geologic model in space.

Table 1: Structural Indices for Magnetic Models used for Depth Estimations

Geologic Model	No. of infinite dimension	Magnetic Structural index
Contact	2(x, y, z)	0
Sill	2(x and y)	1
Dyke	2(z and x-y)	1
Pipe	1(z)	2
Horizontal cylinder	1(x-y)	2
Sphere	0	3

With appropriate choice of structural indices, 3-D Euler deconvolution will lead to clustering of solutions which can be interpreted geologically (Whitehead and Musselman, 2008).). A sill for example can be seen as a cluster of solutions around a curvature. A vertical pipe structure will show as a cluster of solutions around a specific point while an elongated dyke structure will be recognized as a linear trend of solutions. Therefore, using the recommendation of Reid *et al.* (1990), the SI is set to 1 with a maximum depth tolerance of 15% and a window dimension of 5 by 5 units.

The 2-D Spectral Inversion Method

The residual map of the study area was divided into thirty-six (36) blocks of magnetic sections. All the thirty-six sections covered $55km^2$. The thirty-six (36) blocks represent a square grid of 32 by 32 residual field values, which corresponds to half degree to half degree i.e. 0.5^0 by 0.5^0 map. The divisions of residual data/map into 36 spectral sections were done with Oasis montaj and the spectral energies were plotted within it, the *.SPC file obtained were later exported into the Microsoft Excel worksheets one after the other until the total number of 36 spectral (*.SPC) energy files were exported. The Microsoft Excel worksheets file obtained was later used as an input file into a spectral program plot (SPP) developed with Matlab. The total numbers of 36 spectral energies were plotted in Matlab with the developed program. A typical plot of energy against frequency (wavenumber) is as shown in Fig. 5. From the slopes of the plot, the first and the second magnetic source depth was respectively estimated using the relations below:

$$z_1 = -{}^{m_1 L}/_{4\pi} \qquad (4)$$

$$z_2 = -{}^{m_2 L}/_{4\pi} \qquad (5)$$

where m_1 and m_2 are slopes of the first and second segment of the plot, L shows length of the cross-section of anomaly while z_1 and z_2 are first and second depths respectively (Table 2). The coordinates of each spectral block were obtained by summing the values of the bounding latitude and longitude and averaging it. This was used in plotting the spectral energy against frequency as presented in equation 5. 2-D spectral inversion allows for estimation of the depth of an ensemble of magnetized blocks of varying depth, width, thickness and magnetization was also carried out in this study. These depths were established from the slope of the log- power spectrum at the lower end of the total wave number or spatial frequency band. The method allows an estimate of the depth of an ensemble of magnetized blocks of varying depth, width, thickness and magnetization. Most of the approaches used involve Fourier transformation of the digitized aeromagnetic data to compute the energy (or amplitude) spectrum. This is plotted on a logarithmic scale against frequency. The slopes of the segments yield estimates of average depths to magnetic or gravity sources of anomalies. Given a residual magnetic anomaly map of dimensions l x l, digitized at equal intervals, the residual total intensity anomaly values can be expressed in terms of a double Fourier series expression given as:

$$T\,(x, y) = \sum_{n=1}^{N} \sum_{m=1}^{M} P_m^n \, \mathrm{Cos}\left\{\left(\frac{2\pi}{l}\right)(nx + my)\right\} + \mathrm{Sin}\left\{\left(\frac{2\pi}{l}\right)(n - my)\right\} \quad (6)$$

Where, l = dimensions of the block, and is the Fourier amplitude and N and M are the number of grid points along the x and y directions respectively. Similarly, using the complex form, the two-dimensional Fourier transform pair may be written as:

$$G\,(u, v) = \iint_{-\infty}^{\infty} g(e^{-j(u_x + v_y)}\, dx\, dy \qquad (7)$$

And

$$g\,(u, v) = \iint_{-\infty}^{\infty} G(u, v)(e^{j(u_x + v_y)}\, du\, dv \qquad (8)$$

Where, u and v are the angular frequencies in the x and y directions respectively.

The use of this method involved some practical problems, most of which are inherent in the application of the Discrete Fourier Transform (DFT). These include the problems of aliasing, truncation effect or Gibb's phenomenon and the problems associated with even and odd symmetries of the real and imaginary parts of the Fourier transform. However, some of the associated problems were addressed by the software used in the analysis.

RESULTS AND DISCUSSION

The aeromagnetic data of the study area is presented as a total magnetic field intensity map (Fig. 3). The map emphasizes the intensities and the wavelengths of the local anomalies that reveal information on the geometry, strike, contacts between rocks, and intensities of magnetization within the study area. Several anomalies can be referred to distinct magnetic zones. The magnetic intensity values in the study ranges from -78.95 to 127.491 nT. Magnetic anomalies of both short and long wavelengths represented by magnetic highs and lows were revealed on the total magnetic field intensity map of the area. Alternations of regions of high and low magnetic anomalous values were observed on the total field intensity map indicating high and low basement relief respectively. The high basement relief may be interpreted as the crest of regional folds or the roof zone of subsurface intrusive bodies with magnetic signatures ranging between 73.77 to 127.491 nT, whereas the low basement relief with the observed magnetic anomalies of about -78.95 to 7.78 nT may correspond to the trough or areas where the basement may have subsided. Geological map of the study area, according to the work of Balogun (2019) shows that the lithologic unit that has the highest magnetic signatures content with pink and red colour ranging in magnetic susceptibilities from 60.524 to 127.491 nT (Fig. 3) could be migmatite, quartzite, biotite gneiss and silicified quartz. These lithologic units corresponding to magnetic anomalies between 60.57 to 129.58 nT are exposed towards the northwestern, central and southern part of the study area around Oko Erin, Aremu, Omupo, Offa, Edidi and Oyan with pockets and flaggy occurrence in the southern and southeastern part of the study area respectively.

Most of these occurrence trends towards NE-SW direction. Meanwhile, towards the southeastern part of the study area close to Ila Orangun is the undifferentiated Schist which is characterized by yellowish colour showing moderately relatively intermediate magnetic anomalies content. However, pockets of lithologic units were observed mostly around the center of the study area, showing very low magnetic content with magnetic susceptibilities ranging from -87.901 to 32.855 nT which could correlate with rocks of relatively high percentage of mafic minerals such as biotite hornblende granodiorite. The total magnetic field intensity map of the area also revealed prominent linear and curvilinear magnetic anomalies associated with sharp gradients as well as positive and negative closures.

The linear features identified on the magnetic intensity map were interpreted using Gay (1972) criteria which include abrupt termination of linear highs and/or lows, abrupt changes in the linear gradients, linear contour patterns and any combination of the preceding criteria. The high magnetic intensity observed around Oko Erin, Omupo and Ajasse Ipo suggests the existence of deep-seated basement features which confirms that the study area has been subjected to both regional stress and strain fields.

3-D Euler Deconvolution

The result of 3-D Euler Deconvolution analysis was presented in the Fig. 4a as a colour-range symbol map. The Euler solution therefore gave a depth limit of about 1200 m and implies that the structures in the study area have relatively shallow depth. More so, it was observed that the result of the 3-D Euler deconvolution agrees with that of the structural patterns displayed on the THD map but the Euler solution clearly defines the depth and orientations of lineaments present in the study area. Figure 3c shows the superimposed maps. The use of structural index of 1.0 for a wide range of geologic model for dyke/sill revealed standard Euler solution clusters as shown in the maps (Figs.4a – c).

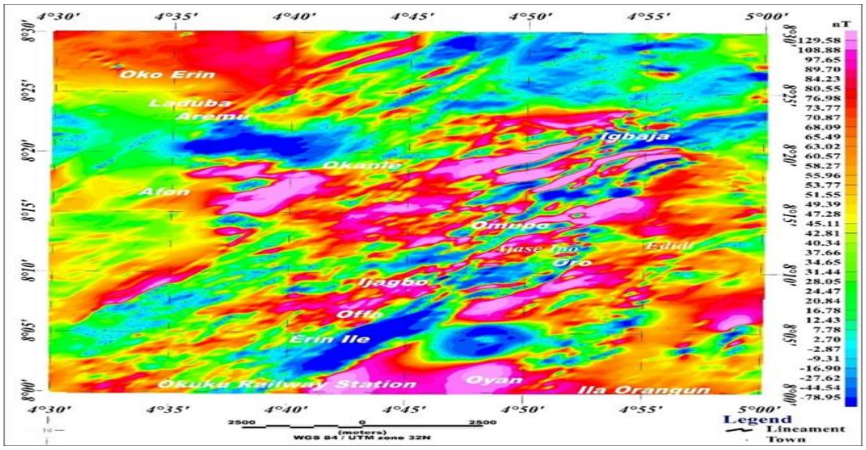

Figure 3: Total Magnetic Intensity aeromagnetic map (TMI) of Ilorin (Sheet 223)

In order to differentiate between the various solutions, unwanted solutions which interfere with proper understanding of the obtained solutions must be removed. Therefore, the elimination of these unwanted solutions determines the choice of depth range used in differentiating the solutions. The interpreted depth ranges for this study ranges from 0 to 800 m which enhances a better comparison of the solutions obtained. Fig. 4a revealed Euler depth range between 200 m to above 800 m, with heavily concentrated clusters of solutions seen around Afon, Okanle and Laduba areas.

Other places where slightly concentrated clusters of solutions exist are Offa, Erinle, Edidi areas and the northeastern part of the study area. This indicates that magnetic dyke/sill is a major geological feature dominating a major part of the study area. There is however a near absence of clusters in the southwestern and central portions of the study area. The results of depth to anomalous basement from this method revealed a high level of agreement with spectral depths. The average basement depth value of 1.2 km interpreted for the study area is in line with results of earlier studies carried out within the study area (Magaji *et al.*, 2025b; Balogun, 2019; Ismaeel *et al.*, 2025).

Magnetic depth from the standard 3-D Euler deconvolution revealed a depth of 0.2km to above 1.10km, which is almost very similar to those obtained elsewhere in the southwestern part of the study area by Lawal (2020) who estimated a depth of 1.6km within Ilorin, Osi, Ado-Ekiti and Omu Aran area. The main magnetic structural trend of NE-SW direction which controls the basement orientation is suspected to be link with Atlantic fracture system (Falebita, 2008; Nuhu, 2009). This trend represents significantly features of the tectonic and structural framework of the basement complex.

Depth Estimation Results

Average radial power analysis identified two main anomaly types which correspond to two (2) distinct layer plot of energy spectrum against frequency (cycle/km) for 36 sections (Fig. 5). They are high amplitude with lower wave number power spectrum which corresponds to relatively deep structures and low amplitude with higher wave number power spectrum that corresponds to shallower sources. The depth range to the various anomalous magnetic bodies estimated from the power spectrum plots of the magnetic field of the study area revealed two-layer depth model (h1 and h2).

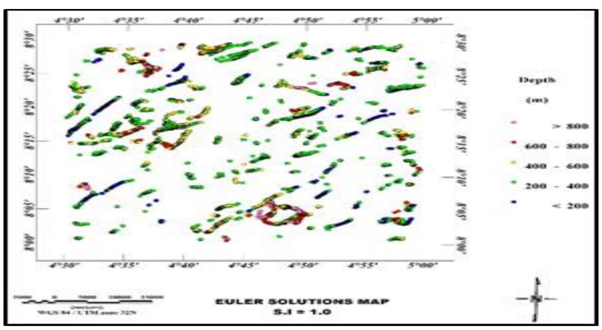

(a)

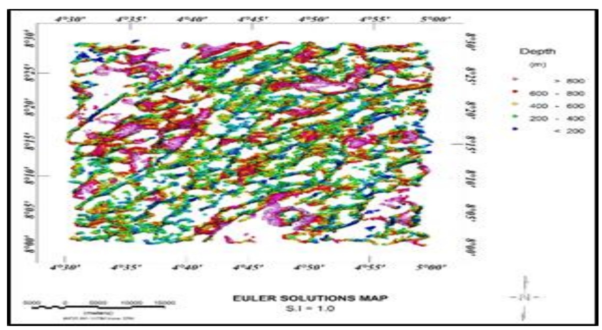

(b)

Figures 4 (a & b): Euler Solution Plot of Ilorin (Sheet 223) (S.I. =1.0) all Solutions, (b) Windowed Solutions

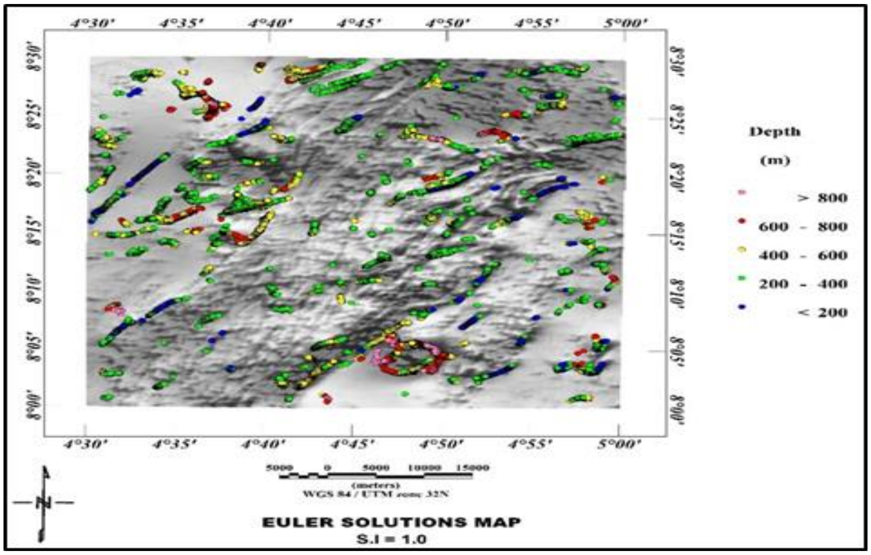

Figure 4c: Euler solution plot of Ilorin (Sheet 223) (S.I. =1.0) windowed solutions on shaded relied of TMI map

The first layer depth (represented by the first segment of the spectrum h1), is interpreted as the depth to the deeper anomalous magnetic sources while the second layer depth (represented by the second segment of the spectrum h2), is interpreted as the depth to the shallower anomalous magnetic sources as seen in Table 1. The map of the first layer (h1) (Fig. 6) varies from 0.380 km to 1.120 km, with an average of 0.728 km. The deeper magnetic anomalies could be attributed to the presence of intrusions of magnetic basement at much deeper depths, lateral discontinuities in the basement and other features differing in magnetic susceptibilities such as dykes, fractures, faults, horsts and grabens within the study area. The second layer depth (h2) map (Fig. 7) varies 0.250 km to 0.480 km, with an average of 0.341 km. The shallower magnetic source could be attributed to the presence of near surface magnetic source which could be sedimentary cover or soil enrichment as a result of weathering. These layers are believed to be as the result of magnetic basement rock, lateral variations in basement susceptibilities, and possibly intra-basement features like faults and fractures probably resulting from tectonism (Balogun, 2022). The magnetic basement depth increases from the northwestern part of the study area to the northern part in the deeper magnetic source (Fig. 6) while the depth to the shallower magnetic sources increases from the northeastern part of the study area to the southern part (Fig. 7). It can be deduced that the basement is shallowest within the southern part of Ilorin around Omupo, Ajase Ipo and Oro. Similarly, the southwestern part of the study area around Okuku is believed to have much thicker sediment pile because the basement is deeper in those areas.

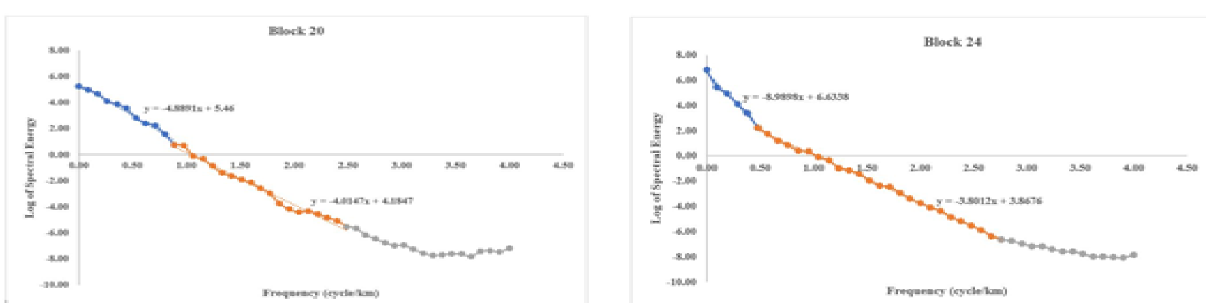

(a) (b)

Figures 5 (a-b): A Typical Plot of Energy Spectrum against Frequency (cycle/km) for blocks 20 and 24

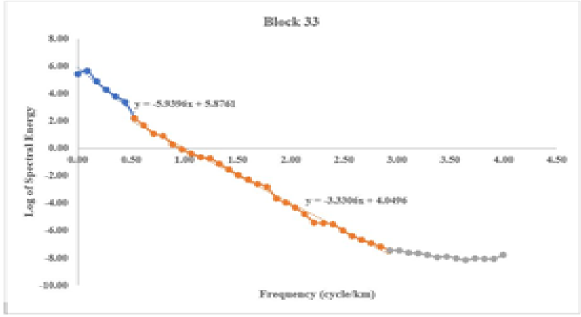

(c)

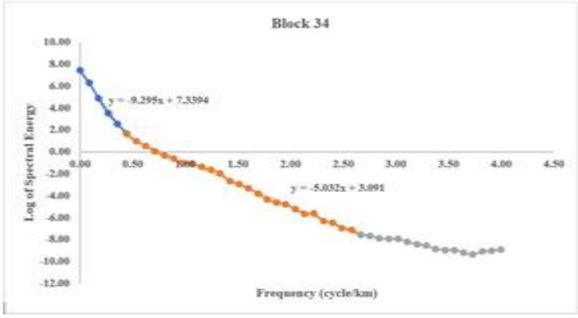

(d)

Figures 5 (c-d): A Typical Plot of Energy Spectrum against Frequency (cycle/km) for blocks 33 and 34

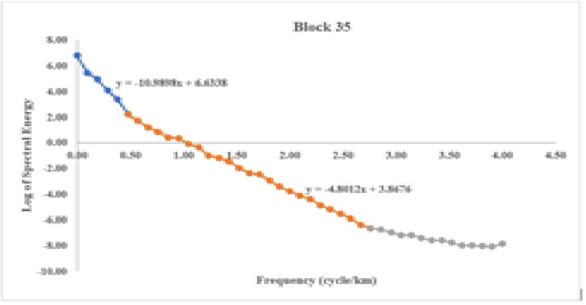

(e)

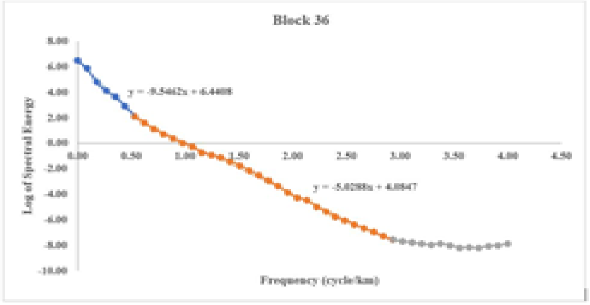

(f)

Figures 5 (e-f): A Typical Plot of Energy Spectrum against Frequency (cycle/km) for sections

Table1: Estimated Depth to the Shallow Depth, $H_1(Km)$ Magnetic Sources and Deep Depth $H_2(Km)$ Magnetic Sources

S/N	SS	$X^{(DMS)}$	$Y^{(DMS)}$	m_1	m_2	$h_1(km)$	$h_2(km)$
1	SS1	004^0 32′30′′	08^0 02′30′′	-3.782	-8.581	0.31	0.69
2	SS2	004^0 37′30′′	08^0 02′30′′	-3.939	-4.808	0.32	0.41
3	SS3	004^0 42′30′′	08^0 02′30′′	-3.814	-13.758	0.30	1.09
4	SS4	004^0 47′30′′	08^0 02′30′′	-3.904	-11.776	0.27	0.62
5	SS5	004^0 52′30′′	08^0 02′30′′	-3.961	-6.279	0.35	0.50
6	SS6	004^0 57′30′′	08^0 02′30′′	-4.920	-9.742	0.39	0.78
7	SS7	004^0 32′30′′	08^0 07′30′′	-4.029	-8.146	0.34	0.65
8	SS8	004^0 37′30′′	08^0 07′30′′	-4.018	-9.493	0.28	0.76
9	SS9	004^0 42′30′′	08^0 07′30′′	-3.764	-8.931	0.36	0.71
10	SS10	004^0 47′30′′	08^0 07′30′′	-4.032	-13.295	0.28	1.06
11	SS11	004^0 52′30′′	08^0 07′30′′	-4.064	-9.342	0.25	0.74
12	SS12	004^0 57′30′′	08^0 07′30′′	-4.008	-10.308	0.33	0.82
13	SS13	004^0 32′30′′	08^0 12′30′′	-3.727	-5.237	0.26	0.42
14	SS14	004^0 37′30′′	08^0 12′30′′	-3.951	-7.020	0.34	0.56
15	SS15	004^0 42′30′′	08^0 12′30′′	-3.926	-5.189	0.36	0.48
16	SS16	004^0 47′30′′	08^0 12′30′′	-3.216	-4.8270	0.28	0.38
17	SS17	004^0 52′30′′	08^0 12′30′′	-3.849	-5.025	0.26	0.40
18	SS18	004^0 57′30′′	08^0 12′30′′	-3.737	-4.809	0.29	0.38
19	SS19	004^0 32′30′′	08^0 17′30′′	-4.824	-5.106	0.35	0.41
20	SS20	004^0 37′30′′	08^0 17′30′′	-4.015	-12.889	0.32	1.11
21	SS21	004^0 42′30′′	08^0 17′30′′	-4.631	-6.1996	0.34	0.49
22	SS22	004^0 47′30′′	08^0 17′30′′	-3.877	-10.840	0.29	0.86
23	SS23	004^0 52′30′′	08^0 17′30′′	-4.031	-11.150	0.32	0.89

S/N	SS	$X^{(DMS)}$	$Y^{(DMS)}$	m_1	m_2	h_1(km)	h_2(km)
24	SS24	004^0 57′30′′	08^0 17′30′′	-3.801	-8.989	0.37	0.72
25	SS25	004^0 32′30′′	08^0 22′30′′	-4.303	-6.716	0.34	0.53
26	SS26	004^0 37′30′′	08^0 22′30′′	-4.425	-10.541	0.35	0.84
27	SS27	004^0 42′30′′	08^0 22′30′′	-4.106	-8.284	0.38	0.66
28	SS28	004^0 47′30′′	08^0 22′30′′	-3.779	-8.581	0.32	0.52
29	SS29	004^0 52′30′′	08^0 22′30′′	-3.782	-8.508	0.28	0.68
30	SS30	004^0 57′30′′	08^0 22′30′′	-3.943	-11.037	0.31	0.88
31	SS31	004^0 32′30′′	08^0 27′30′′	-3.413	-9.415	0.29	0.75
32	SS32	004^0 37′30′′	08^0 27′30′′	-3.156	-6.377	0.25	0.51
33	SS33	004^0 42′30′′	08^0 27′30′′	-3.331	-5.939	0.37	0.48
34	SS34	004^0 47′30′′	08^0 27′30′′	-5.032	-9.295	0.40	0.74
35	SS35	004^0 52′30′′	08^0 27′30′′	-4.801	-10.989	0.38	0.87
36	SS36	004^0 57′30′′	08^0 27′30′′	-5.029	-9.5462	0.40	0.76

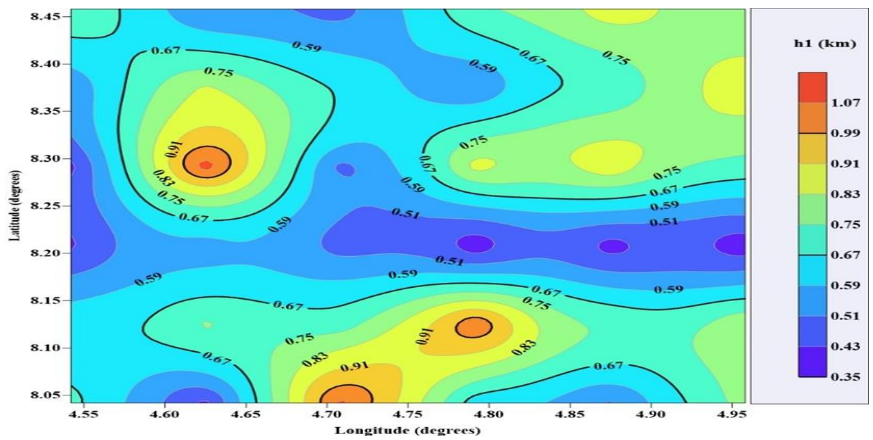

Figure 6: Deeper Depth Anomalies (H1) Map of the Study Area

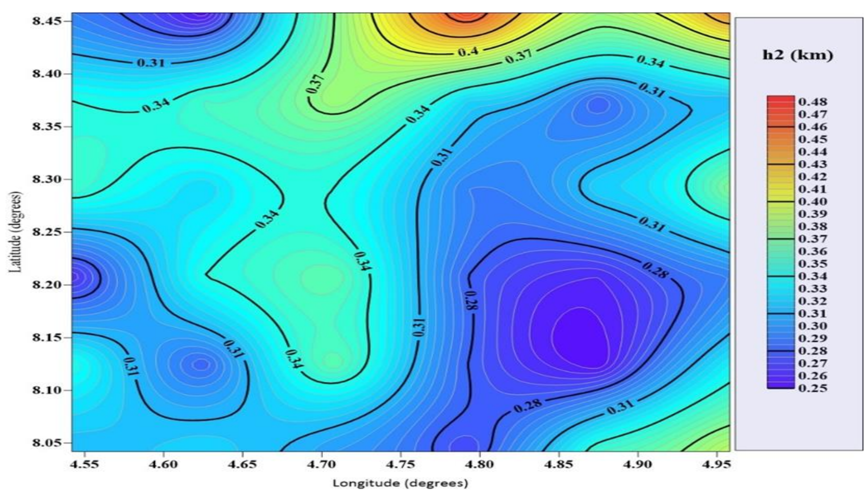

Figure 7: Shallower Depth Anomalies (H1) Map of the Study Area

CONCLUSION

An aeromagnetic data of Sheet 223 was used to interpret subsurface structures and magnetic source depths of Ilorin Kwara State. Two different standard techniques based on the frequency analysis of the magnetic field (2D spectral analysis and 3D Euler deconvolution) were established. 2-D spectral analysis estimated the magnetic basement depths (shallower and deeper source depths) of causative bodies with an average of 0.728 km for deeper source and 0.341 km for shallower source. The geometry form and depth of the subsurface features with the structural index of 1 were determined by 3D Euler deconvolution. More concentration clusters of euler solutions were seen around Afon, Okanle and Laduba areas with depth limit of about 200 m which depicts the shallow sources. It is thereby recommended to carry-out ground truthing, geochemical analysis or integration of other geophysical methods like radiometric, gravity or electrical resistivity to follow-up the results.

REFERENCES

Abaa, S. I. (1983). The structure and petrography of alkaline rocks of the Mada Younger Granite Complex, Nigeria. Journal of African Earth Sciences 3: pp. 107–113.

Balogun, O. B. (2019). Tectonic and structural analysis of the Migmatite–Gneiss–Quartzite complex of Ilorin area from aeromagnetic data. NRIAG Journal of Astronomy and Geophysics, 8(1), https://doi.org/10.1080/20909977.2019.1615795.

Chibuike A., Paulinus N., Nnaboa, C. C., Ania, I. A., Obasib, P. N. and Obasia, D. C. (2022). Application of Ground Magnetic Method for Delineation Subsurface Structural Control on Sulphide Ore Deposit in Benue Trough; A Case Study of Ikenyi Izzi, Earth Sciences Malaysia (ESMY) DOI: http://doi.org/10.26480/esmy.01.2023.07.19

Falebita DE (2008) Integrated geophysical mapping of the Ifewara transcurrent fault system, Nigeria. J Afr Earth Sci 52:161–166.

Folorunso, I. O., Magaji, Y., Ajadi, J and Umar, I. (2024). Application of Euler and Werner deconvolution techniques in delineating tin deposit in Okeso area, Southwestern, Nigeria. Proceedings of the Nigerian Society of Physical Sciences 1, 96.

Gay S. P. (1972). Fundamental characteristics of aeromagnetic lineaments: Their geological significance and tectonic significance to geology, Salt Lake City, Utah. American Stereo Map. 94.

Gunn P. J. (1997). Application of aeromagnetic surveys to sedimentary basin studies. AGSO Journal of Australian Geology and Geophysics.17 (2):133-144.

Ismaeel, F.O., Yusuf, M., Olarewaju, A.H., Salaudeen, S.A., Obalalu, A.M., Khan, U. andAlsawah, G.A. (2025). Muscovite ore exploration using 3-D Euler deconvolution andtotal horizontal gradient of magnetic anomalies in Eleeku, Northcentral, Nigeria. Z Angew Math Mech. 105, e70247. https://doi.org/10.1002/zamm.7024.

Liu, X. (2003). On the use of different methods for estimating magnetic depth. The Leading Edge. 2003; 22:1090–1099.

Magaji, Y. and Sanusi, Y. A. (2021). Evaluation of hydrocarbon prospect in Lema area, western parts of Sokoto Basin, Nigeria, based on analysis of high-resolution aeromagnetic data. Quest Journals Journal of Research in Environmental and Earth Sciences, 7(4), 46–61.

Magaji, Y., Folorunso O. I., Salaudeen, A. S., Olajide, A. T. and Wahab, O. F. (2025a). Structural and Mineralization Mapping of Muscovite Ore Deposit in Eleeku Southwestern, Nigeria. FUDMA Journal of Sciences (FJS), 9(10), 277-289.

Magaji, Y., Folorunso O. I., Wahab, O. F. and Salaudeen, A. S. (2025b). Aeromagnetic Perspectives on Basement Morphology and Depth beneath Ilorin Metropolis, Southwestern, Nigeria. Dutse Journal of Pure and Applied Sciences (DUJOPAS), 11(4a), 143-153.

Matheis, G., Caen-Vachette, M. (1983). Rb-Sr isotopic study of rare-metal bearing and barren pegmatites in the Pan-African reactivation zone of Nigeria. J. Afr. Earth Sci. 1, 35-40.

Nabighian, M.N. (1972). The analytic signal of two-dimensional magnetic bodies with polygonal cross-section: its properties and use for auto mated anomaly interpretation. Geophysics. Society of Exploration Geophysicists 37(3):507–517.

Nuhu, G.O. (2009) Geology and mineral resources of Nigeria, Lecture Notes in Earth Sciences. 120, Springer-Verlag, Berlin Heidelberg.

Rahaman, M. A. (1988). Recent advances in the study of the Basement Complex of Nigeria. In Precambrian geology of Nigeria (pp. 11–43). Geological Survey of Nigeria.

Rahaman, M. A. (1989). Review of basement geology of Southwestern Nigeria. In C. A. Kogbe (Ed.), Geology of Nigeria (2nd ed., pp. 39–56). Rock View Ltd.

Reid, A.B. and Thurston, J.B. (2014) the structural index in gravity and mag netic interpretation: errors, uses and abuses. Geophysics 79(4): J61 J66. http://doi.org/10.1190/GEO2013-0235.1

Reid, A.B., Alisop, J.M., Granser, H., Millett, A.J. and Somerton, I.W. (1990) Magnetic interpretations in three dimensions using Euler deconvolution. Geophysics 55:80–91

Olatunji, S. and Warith, A.A. (2022). Werner Deconvolution Technique for the Interpretation ofResidual Aeromagnetic Anomalies of Igbeti Schist Belt; Implication for MarbleExploration. Indonesian Journal on Geoscience. http://ijog.geologi.esdm.go.id. 9(2). 209-217.

Opara AI, Onyewuchi RA, Selemo AOI, Onyekuru SO, Ubechu BO, Emberga TT, Ibim DF, Nosiri OP. Structural and tectonic features of ugep and environs, calabar flank, Southeastern Nigeria: Evidences from Airborne Magnetic and Landsat- ETM data. Mitteilungen Klosterneuburg Journal. 2014; 64.

Saada AS (2016). Edge detection and depth estimation of Galala El Bahariya Plateau, Eastern Desert-Egypt, from aeromagnetic data. Geomech Geophys Geo-energy Geo-resour 2: 25–41.

Saheed, O. & Magaji, Y. (2022). Analysis of High-Resolution Aeromagnetic Data over Parts of Sokoto Basin, North-West Nigeria", A Journal of Engineering. https://www.researchgate.net/publication/358452877.

Salawu NB, Olatunji S, Orosun MM, Abdulraheem TY (2019) Geophysical inversion of geologic structures of Oyo Metropolis, Southwestern Nigeria from airborne magnetic data. Geomech Geophys Geo-energy Geo-Resour 5: 143–157.

Thompson D.T. (1982) "EULDPTH: A new technique for making computer-assisted depth estimates from magnetic data", Geophysics *47* 31-37. https://www.sciencedirect.com/S1002070508600266.

Udensi EE, Osazuwa IB. Spectral determination of depth to buried magnetic rocks under the nupe basin, Nigeria. Nigerian Association of Petroleum Explorationists Bulletin. 2004; 17(1): 22-27.

Whitehead, N. and Musselman, C. (2008). Montaj gravity/magnetic interpretation: Processing, analysis and visualization system for 3-d inversion of potential field data for oasis montaj v6.3, Geosoft Incorporated, 85 Richmond St. W., Toronto, Ontario, M5H 2C9, Canada.